

Highly selective fluorescent chemosensors for cadmium in water

Thorfinnur Gunnlaugsson,^{a,*} T. Clive Lee^b and Raman Parkesh^a

^a*Department of Chemistry, Trinity College Dublin, Dublin 2, Ireland*

^b*Department of Anatomy, Royal College of Surgeons in Ireland, St. Stephen's Green, Dublin 2, Ireland*

Received 1 February 2004; revised 5 August 2004; accepted 19 August 2004

Available online 1 October 2004

Abstract—The design, synthesis and photophysical evaluation of two new chemosensors **1** and **2** is described for the selective detection of Cd(II) in water at pH 7.4. Both are based on the use of aromatic iminodiacetate receptors that connected to an anthracene fluorophore by covalent methyl spacers. These are highly water-soluble sensors where the fluorescence is ‘switched off’ between pH 3–11, due to photoinduced electron transfer (PET) quenching of the anthracene excited state by the receptor. Upon protonation of the receptor, the emission was however, ‘switched on’. From these changes pK_as of 1.8 and 2.5 were determined for **1** and **2** respectively. Both showed good selectivity for Cd(II) over competitive ions such as group II and Zn(II), Cu(II), Co(II). For **1**, having a single receptor, only a weak monomer anthracene emission was observed for the free sensor at pH 7.4 (HEPES buffer, 135 mM NaCl). Upon Zn(II) titration, a broad red shifted emission occurred, centred at 468 nm. In the presence of Cd(II), a similar red shifted emission was also observed, however, this time centred at 506 nm. In contrast to these results, the fluorescence of **2** in the presence of Zn(II) gave rise to typical monomeric anthracene emission, due to suppression of PET, that is, the anthracene emission was ‘switched on’. Nevertheless, in the presence of Cd(II) a broad emission centred at 500 nm was observed, similar to that seen for **1**. These ion induced long wavelength emission bands were assigned to the formation of charge-transfer complexes (exciplexes) between the anthracene moieties and the ion-receptor complexes. Importantly, for both **1** and **2**, a selective detection of Cd(II) was possible, even in the presence of Zn(II).

© 2004 Elsevier Ltd. All rights reserved.

1. Introduction

The development of luminescent sensors lies at the heart of supramolecular chemistry.¹ Several research groups have recently reviewed work in this area.^{1–3} We have developed various types of luminescent devices, some of which have been developed as sensors for ions and molecules. These include fluorescent⁴ and colorimetric⁵ sensors as well as lanthanide luminescent⁶ chemosensors for cations such as Li⁺, Na⁺, K⁺, Cu(II) and Zn(II) and anions such as F[−], AcO[−], H₂PO₄[−], pyrophosphate, carboxylates, and aromatic carboxylates such as salicylic acid. The main driving force for this work has been the increased use of chemosensors for medical diagnostics,⁷ and in particular for critical care analysis.⁸ During the course of our research we initiated an investigation into developing luminescent sensors for metal ions such as Cd(II), but only a few examples of sensors for Cd(II) have been reported.⁹ Furthermore, those reported to date for Cd(II) detection suffer from several drawbacks such as low aqueous solubility, poor sensitivity and selectivity, as well as unsuitability for use in the physiological pH range. The need for developing ideal chemosensors for Cd(II), that

satisfy the aforementioned criteria is thus currently of great importance. In this paper we describe the design, synthesis and the photophysical evaluation of two novel fluorescent sensors, **1** and **2** for the selective sensing of Cd(II) under physiological pH conditions.¹⁰

Cadmium, an ion that poses an increasing environmental and health risk, has a naturally low abundance in nature (0.1–0.5 ppm).¹¹ However, cadmium levels as high as 500 ppm have recently been reported to accumulate in sedimentary rocks and marine phosphates and phosphorites.¹² One of the reasons for this is that Cd(II) is used in Ni–Cd batteries, as well as in fertilisers.¹³ In the former, Cd(OH)₂ is used as one of the two principal electrode materials.¹⁴ Even though Li⁺ based batteries are now becoming more common, the disposal of unused Ni–Cd batteries is, and will be, a major environmental problem, particularly since cadmium has profound biological effects such as inducing renal dysfunction, reduced lung capacity and emphysema.¹⁵ The tendency of this toxic ion to accumulate in organs such as the kidneys, hippocampus, thyroid and spleen, results in severe physiological effects.¹⁶ Although only about 0.4% of the total amount of ingested cadmium is retained in the human body, recent studies indicate that high toxic levels of Cd(II) in the kidney and thyroid glands can occur, particularly in miners.¹⁷

Keywords: Chemosensors; Fluorescent; PET; Supramolecular chemistry.

* Corresponding author. Tel.: +35316083459; fax: +35316712628; e-mail: gunnlaout@tcd.ie

Furthermore, it has recently been suggested that Cd(II) affects bone demineralisation by activating the osteoclast bone cells.¹⁸ Moreover, cadmium is also thought to be a potential carcinogen.¹⁹ All of these factors make the detection and quantification of Cd(II) a vital area of research. With this in mind we set out to develop the two chemosensors **1** and **2**. We designed these sensors on the fluorophore-spacer-receptor and the receptor-spacer-fluorophore-spacer-receptor models developed by de Silva et al. for PET sensors.²⁰ Here we give a full account of our effort.¹⁰

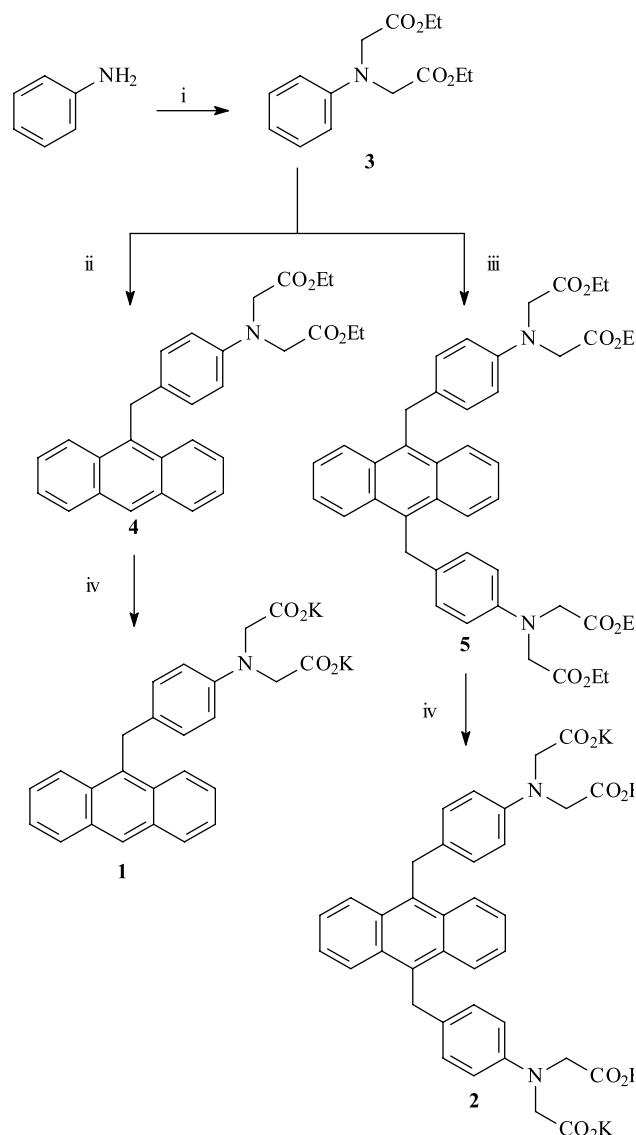
2. Results and discussion

2.1. Synthesis and characterisation of **1** and **2**

For the two chemosensors **1** and **2**, we selected anthracene as a fluorophore, and a simple aromatic iminodiacetate as the receptor. The reasons for this were twofold. First, the photophysical properties of anthracene in PET sensors is well established.^{3,20} Secondly, the aniline based receptor could be used under physiological pH conditions as the nitrogen receptor moiety would only protonate under highly acidic conditions.²¹ Moreover, this simple design would overcome any competitive binding of any other physiologically important cations such as Mg^{2+} and Ca^{2+} .²¹ The use of potassium salts of the carboxylates would impart high water solubility to **1** and **2**. In the case of **2**, we predicted that the presence of two receptor units would statistically increase any PET rate quenching from the receptor to the excited singlet state of the anthracene, resulting in effective luminescent switching, where the emission would only be switched on in the presence of Cd(II).

The synthesis of **1** and **2** is shown in Scheme 1. It began with the synthesis of the iminodiester receptor **3**, by reacting aniline with ethyl bromoacetate, using potassium dihydrogen phosphate as a base in CH_3CN in 89% yield. The two sensors were made in two steps from this intermediate. For **1**, this was achieved by Friedel–Crafts alkylation of **3** with 9-chloromethylantracene (which was made in two steps from 9-anthraldehyde by reduction followed by chlorination). This alkylation was very successful, giving the desired product **4** in 70% yield using AlCl_3 in CH_3CN , whereas using ZnBr_2 as catalyst resulted in a low yield of only 15%. The final product was purified using silica flash column chromatography using ethyl acetate:hexane (2:3) as eluant. In an analogous way, **2** was made by reacting 2 equiv of **3** with 9,10-bis(chloromethyl)anthracene (made by chloromethylation of anthracene in a single step),²⁴ yielding the tetraester **5**, in 72% yield, after purification by flash column chromatography using ethyl acetate:hexane (2:3) as eluant. The final products were obtained by alkaline ester hydrolysis of **4** and **5** using aqueous KOH in refluxing MeOH solution, yielding **1** and **2** in 92 and 90% yields respectively after precipitation from the cold solution.

The structures of **1**–**4** were confirmed by the usual spectroscopic methods (see the Section 4). In the ^1H NMR of **4**, a singlet at 8.4 ppm and two multiplets at 8.21–8.24 and 8.02–8.05 ppm, respectively were attributed to the anthracene protons, whereas two doublets at 6.98 and



Scheme 1. The synthesis of **1** and **2** from aniline. (i) CH_3CN , KI, K_2HPO_4 , $\text{BrCH}_2\text{CO}_2\text{Et}$, reflux; (ii) 9-chloromethylantracene, AlCl_3 , CHCl_3 , reflux; (iii) 9,10-bis(chloromethyl)anthracene, KOH, H_2O , MeOH, reflux.

6.47 ppm were observed for the phenyl protons. In comparison, the ^1H NMR of **1** showed two doublets for the phenyl protons at 6.20 and 6.82 ppm, respectively. The electrospray mass spectrum (ESMS) showed a peak at 476 mass units for $\text{M} + \text{H}^+$ (100%). In the ^1H NMR of **5**, the phenyl protons appeared as doublets at 6.50 and 7.01 ppm and a singlet was observed at 4.95 ppm for the two methyl spacers. The symmetrical nature of the molecule was further supported by the ^{13}C NMR in which only 13 carbon resonances were observed. Furthermore, the ESMS spectrum gave a peak at 733 mass units for $\text{M} + \text{H}^+$. After alkaline hydrolysis of **5** the ^1H NMR spectrum of **2** (Fig. 1) showed two double–doublet resonances for the anthracene protons at 8.31–8.29 ppm and at 7.45–7.42 ppm whereas the phenyl protons were observed as two doublets at 6.91 and 6.28 ppm. The two methyl spacers appeared as a singlet at 4.86 ppm and the two methyl iminodiester spacers as a singlet at 4.86 ppm. The ^{13}C NMR gave, as expected, rise to only 11 resonances.

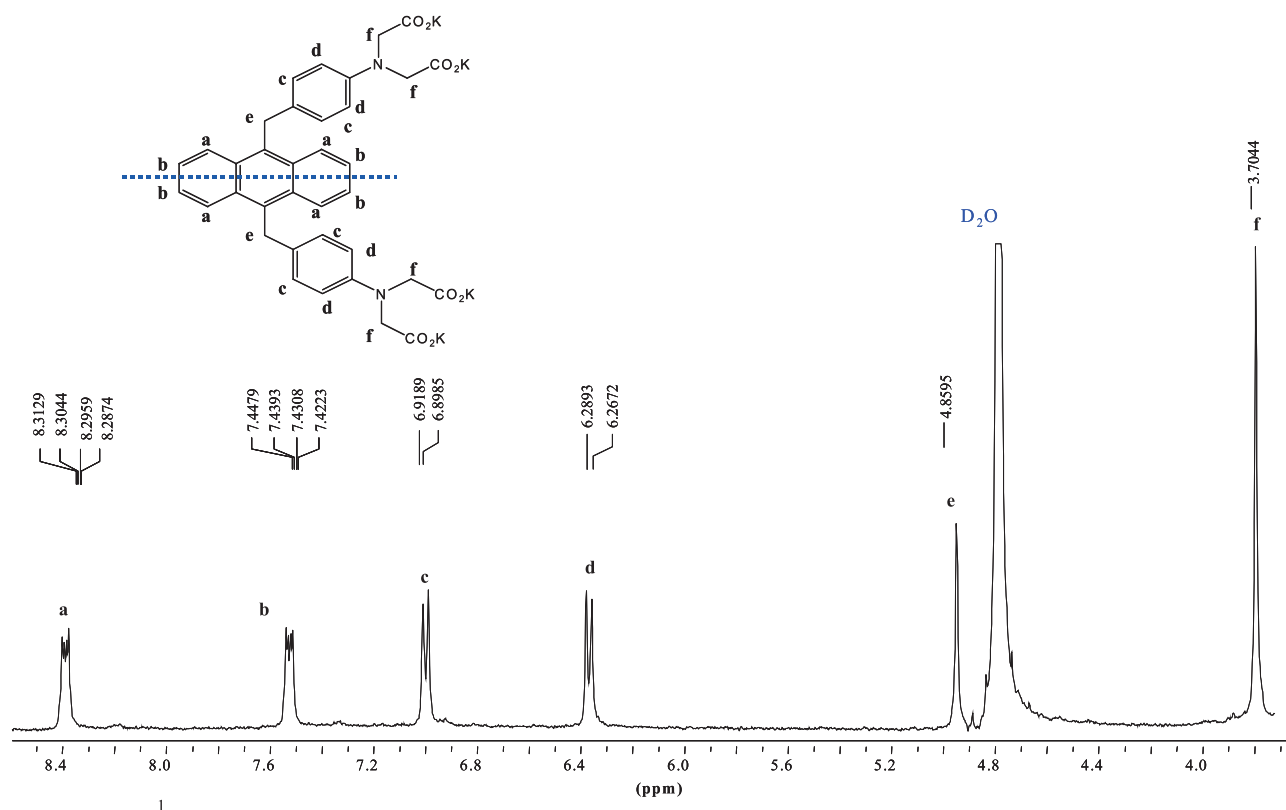


Figure 1. The ^1H NMR of **2** (D_2O , 400 MHz). The appropriate resonances have been assigned as a–f.

2.2. Ground and excited state evaluation of **1** and **2**

The photophysical properties of the two chemosensors **1**, and **2** were evaluated in water and in pH 7.4 HEPES buffered solution in the presence of 0.135 M of NaCl to maintain constant ionic strength.

2.3. The effect of pH

We first evaluated the pH response of **1** and **2** in water. The absorption spectra of **1** exhibited five main absorption bands centred at 314, 337, 365, 385 and 402 nm ($\epsilon = 17.1 \times 10^3 \text{ M}^{-1} \text{ cm}^{-1}$). The absorption spectra of **1** as a function of pH is shown in Figure 2. When an alkaline solution of **1** was titrated with acid, no absorption shifts were seen in the positions of the above mentioned bands. However, a small decrease in the absorption intensity ($< 5\%$) was observed. This was most likely due to the electronic effect observed between the anthracene fluorophore and positively charged aniline moiety upon protonation (through space). These small effects are well known and signify that no significant ground state interactions occur between the fluorophore and the receptor, due to the presence of the covalent spacer. The absorption spectra of **2** as a function of pH were recorded in a similar manner. The absorption spectra of **2** showed four absorption bands at 343, 362, 381 and 402 nm ($\epsilon = 18.6 \times 10^3 \text{ M}^{-1} \text{ cm}^{-1}$) respectively. The absorption spectra generated during the pH titration showed only a negligible decrease in the intensity similar to that seen for **1** in Figure 2. This shows that under these conditions only minor ground state interactions take place between the receptors and the anthracene moiety, confirming the insulating role of the two methylene spacers.

In contrast to the above changes the fluorescence emission of **1** and **2** was substantially changed upon protonation of the amino moiety of the receptors ($\lambda_{\text{ex}} = 381 \text{ nm}$). For **1** in basic solution (pH ~ 12), the fluorescence was so minor that it can be said that the emission was switched off. This is due to PET quenching from the receptor to the excited state of the fluorophore. However, upon titration with acid, a gradual increase was observed for the anthracene emission, which had three characteristic bands centred at 392, 415 and 439 nm and a weak shoulder at 466 nm respectively. This fluorescence enhancement was approximately 60 fold. The increase in fluorescence is due to the protonation of the tertiary nitrogen atom of the receptor moiety, resulting in a decrease in the reduction potential of the receptor, which is typical PET behaviour. This prevents electron transfer from the receptor to the excited state of the anthracene, thus switching the emission on. Similar results were observed for **2** ($\lambda_{\text{ex}} = 385 \text{ nm}$), as seen in Figure 3. In basic solution, the fluorescence of **2** was quenched, and in the pH range of pH = 3.5–12 virtually no emission was observed. However, at around pH 3.4, a broad band centered at 470 nm appeared with an increase in the emission intensity (Fig. 3, insert). Upon further acidification, between pH ~ 3.3 –1.0, the normal anthracene emission with four main emission bands at 405, 428, 454 and 480 nm, respectively was observed with concomitant increase in the fluorescence intensity of ca. 600 fold.

We investigated these changes in some detail for **2**. Our studies revealed that from pH 12–3.5, the fluorescence of the anthracene moiety is efficiently quenched via a PET process from the receptors to the excited singlet state of the anthracene. However, as the pH is decreased protonation of

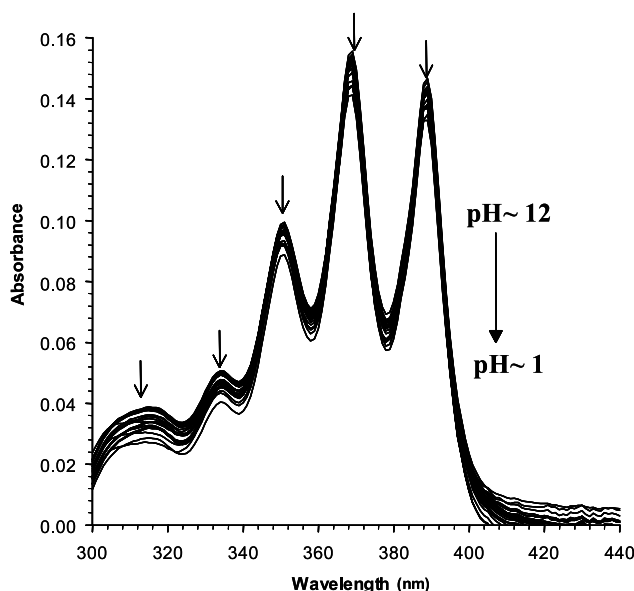


Figure 2. The changes in the absorption spectrum of **1** upon titration an alkaline solution of **1** with diluted acid.

the tertiary nitrogen of one receptor takes place, which causes a weak charge transfer (CT)²³ interaction between the protonated receptor and the anthracene fluorophore. This resulted in a charge transfer band at 470 nm. When the pH is decreased further, both receptors become protonated. These results in a repulsive interaction (RI), and to minimise it the receptors move as far apart as possible in space. Consequently, typical anthracene emission is observed in the pH range of 3.3–1. We were unable to determine more than one pK_a from the changes, Figure 4. The reason for this is most likely due to the fact that the changes in fluorescence emission correspond to the protonation of only one of the two receptors. Lippard et al. have reported similar observations in the case of fluorescein based sensors for Zn(II) ions, where the sensor also had two receptor moieties that could be protonated.²²

Plotting the changes in the fluorescence emission as a function of pH resulted in a sigmoidal curve that changes over two pH units for both sensors. This pH dependent fluorescence behaviour is a typical ‘on-off’ PET sensor characteristic, indicating a simple acid-base equilibrium and one to one binding. The fluorescence intensity changes at 415 nm versus pH are shown for **2** in Figure 4. These, and the changes at any other wavelength, can be used to determine the pK_a of the protonation of the nitrogen moiety. Data fitting analysis of the emission intensity changes at 404, 428 and 454 nm respectively resulted in pK_a values of 2.4, 2.3 and 2.8 providing an average pK_a value of 2.5 ± 0.1 for **2**. Similarly for **1**, the changes at 392, 415 and 439 nm gave pK_a values of 1.75, 1.74 and 2.0 (± 0.1), providing an average pK_a of 1.83 ± 0.1 for the protonation of the aniline receptor in **1**. This makes both **1** and **2** particularly attractive chemosensors for both physiological and environmental monitoring of Cd(II), for instance in highly acidic soils

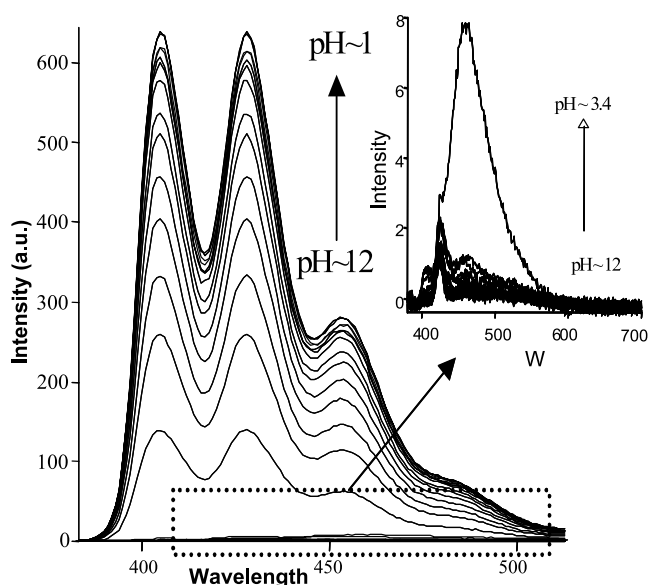


Figure 3. The changes in the fluorescence emission spectra of **2** upon acidification. Inserted are the changes observed between pH 3.4 and 12.

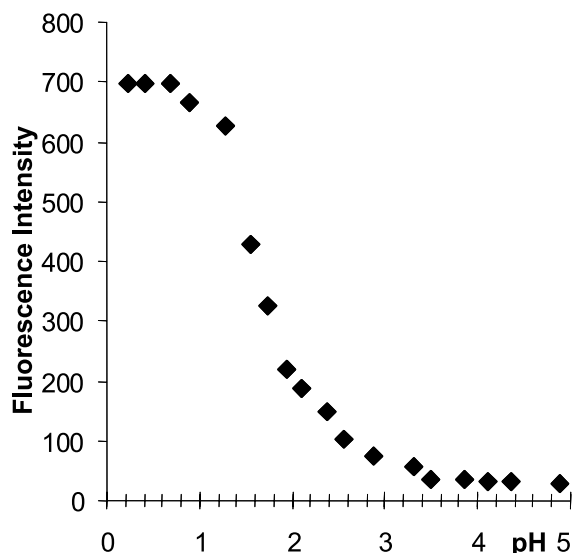


Figure 4. The plot of fluorescence intensity versus pH for **1** at 415 nm. Fitting of these data points using non-linear regression gave the pK_a .

where the pH 3–4 can be reached. Similarly, the pH titrations of the two esters **4** and **5** switched the fluorescence on for both of these molecules upon protonation of the aniline amine.

2.4. The effect of group II and transition metal ions

The ability of **1** and **2** to recognise group II and various transition metal ions was investigated at pH 7.4 in buffered HEPES solution in the presence of 0.135 M of NaCl. We first evaluated the ability of **1** and **2** to recognise group II cations. The changes in the fluorescence emission spectra of **1** are shown in Figure 5 for titration with Ca^{2+} . As can be seen from this titration, the emission is very low in comparison to the changes seen in the pH titration (Fig. 3). The fluorescence is only minor and can be considered as being switched off (identical experimental settings were used for both measurements). Furthermore, no significant changes occurred upon titration of **1** with Ca^{2+} . In fact, even at high concentrations (0.01 M) of Mg^{2+} or Ca^{2+} , no significant spectral changes were observed in either the absorption or the fluorescence emission of the two sensors. This indicates that the receptors in these sensors were not coordinating significantly to these ions to prevent quenching by the receptors.²¹

We next evaluated the response of **1** and **2** towards various transition metal ions such as Co(II), Ni(II), Cu(II), Zn(II), Cd(II) and Hg(II) (as their Cl^- , NO_3^- or ClO_4^- salts). Of these, only Zn(II) and Cd(II) gave rise to any significant changes in the fluorescence emission spectra and the absorption spectra. For **1**, the changes in the fluorescence spectra ($\lambda_{\text{ex}}=370$ nm) upon titration with Zn(II) are shown in Figure 6. We foresaw that the coordination of the receptor (via the nitrogen lone pair and the two carboxylates) would, in a similar way to the protonation of the amino moiety, increase the oxidation potential of the receptor and prevent PET quenching. However, as can be seen from Figure 6, the monomeric anthracene emission was not switched on in an analogous way as previously shown for the pH titration in

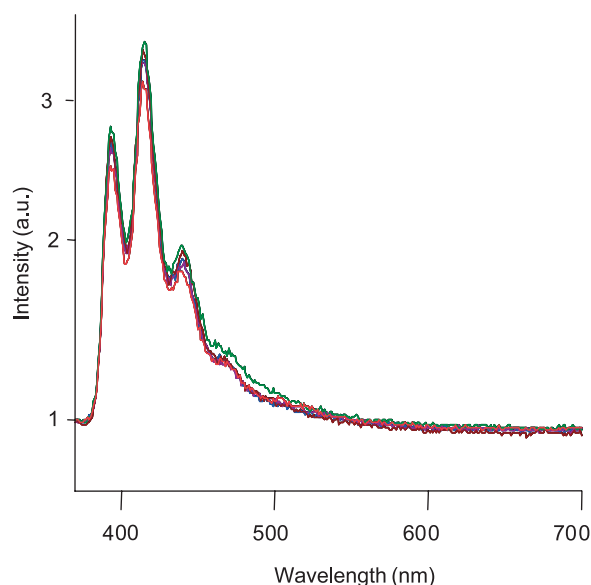


Figure 5. The changes in the fluorescence emission of **1** at pH 7.4, in 0.135 M NaCl, upon titration with Ca^{2+} , $[\text{Ca}^{2+}]=0 \rightarrow 0.01$ M.

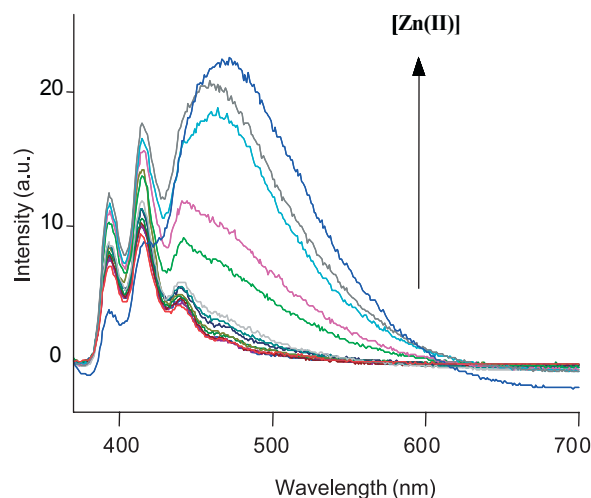


Figure 6. The changes in the fluorescence emission spectra of **1** upon titration with Zn(II).

Figure 3. Here, however, the monomeric anthracene emission was only slightly enhanced upon ion recognition, with the concomitant formation of a new red shifted broad emission band centred at 468 nm. Unlike that seen for the protonation previously, the fluorescent enhancement was much smaller for these changes. The affiliated changes in the absorption spectra were also interesting, as at low and medium concentration of Zn(II) the classical anthracene absorption bands were observed at 335, 350, 365 and 389 nm. Furthermore, these were only slightly reduced in intensity upon Zn(II) titration. Hence the classical PET behaviour was observed. However, at higher Zn(II) concentrations (~ 2 mM) dramatic shifts ($\Delta\lambda=14$ nm) were observed in the absorption bands, which now became centred at 360, 376 and 404 nm, respectively. In conjunction with the changes in the fluorescence emission spectra (Fig. 6), one can deduce that these changes are due the formation of an intramolecular charge-transfer complex²³ (intramolecular exciplex) between the cation-bound acceptor and anthracene donor (see later) (Fig. 7).²⁴

In comparison to these results we carried out an identical titration using **2**. The changes in the absorption spectra of **2** at low and high concentrations of Zn(II) are shown in Figure 8. Here it is clear that no major changes took place upon titration of **2** with Zn(II), with the three absorption bands being shifted by only 2–3 nm. Hence, one can conclude that in comparison to **1**, there are no major ground state interactions occurring between the fluorophore and the receptor. The corresponding changes in the fluorescence emission spectra are shown in Figure 9. They clearly demonstrate that the monomeric emission of the anthracene fluorophore is switched on, similar to that seen earlier for the pH titration. This indicates that the Zn(II) ion was able to coordinate to the carboxylates, as well as the aniline nitrogen and hence increase the oxidation potential of the receptors in a usual PET fashion. For these changes a fluorescence enhancement factor of several hundreds was observed. Most importantly, the Zn(II) recognition does not lead to any charge transfer interactions as seen previously for **1**. Hence, **2** is behaving as a typical PET sensor for Zn(II). A likely reason for this difference could be that the

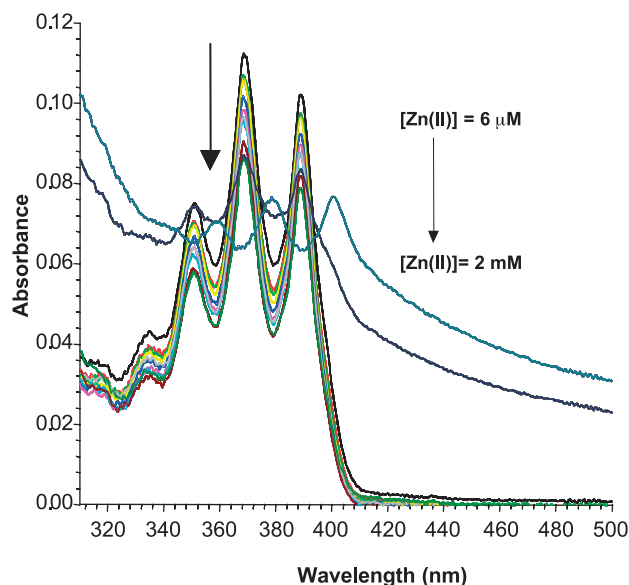


Figure 7. The changes in the absorption spectra of **1** upon titration with Zn(II).

Zn(II) binding forces the receptor to further away from the anthracene fluorophore possibly due to steric effects. However, we have not been able to obtain reliable experimental proof for this.

We were able to evaluate the affinity of both **1** and **2** for Zn(II) by plotting the relative intensity changes at 468 and 415 nm for **1** and **2** respectively, as a function of pZn ($\text{pZn} = -\log [\text{Zn(II)}]$). For both, a sigmoidal curve was observed, which switched on over two logarithmic units between $\text{pZn} \sim 5$ –3. This can be seen in Figure 10 for **2**. Hence, these binding interactions can be determined to be due to 1:1 binding between the two receptors of **2**, and Zn(II). This was indeed confirmed by using the Job plot method. From these changes a binding constant $\log \beta$ of $3.8 (\pm 0.1)$ was determined. Similarly, for **1**, a $\log \beta$ of $3.8 (\pm 0.1)$ was determined. Hence, both sensors have the same

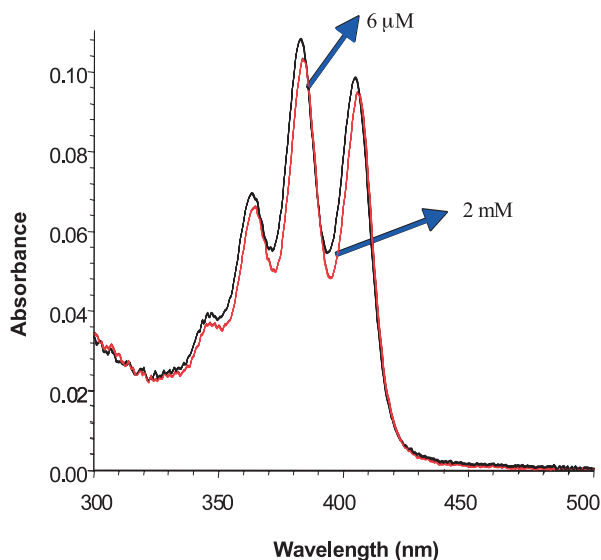


Figure 8. The changes in the absorption spectra of **2** at low and high concentration of Zn(II).

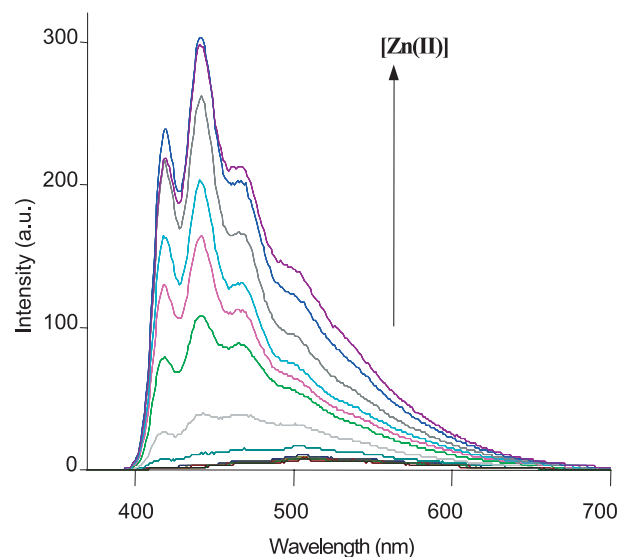


Figure 9. The changes in the fluorescence emission spectra of **2** upon titration with Zn(II).

affinity for Zn(II). We were unable to obtain a reliable binding constant from the absorption spectrum of **1**, as these changes were too small to give accurate binding.

In a similar manner we evaluated the affinity of **1** and **2** for Cd(II). The absorption response of **1** to Cd(II) was quite similar to that observed in the Zn(II) titration. Here, three anthracene absorption bands were observed at 350, 365 and 389 nm, and a small decrease in the absorption intensity was observed upon addition of Cd(II). However, at higher concentrations of Cd(II), the absorption spectra was gradually shifted to longer wavelengths with absorption maxima at 360, 376 and 406 nm, with the formation of isosbestic points at 370, 382 and 395 nm, respectively. As explained earlier, these latter changes are probably due to the charge transfer interaction occurring between the anthracene and receptor-Cd(II) complex. From these changes we were able to determine $\log \beta$ of $4.0 (\pm 0.1)$.

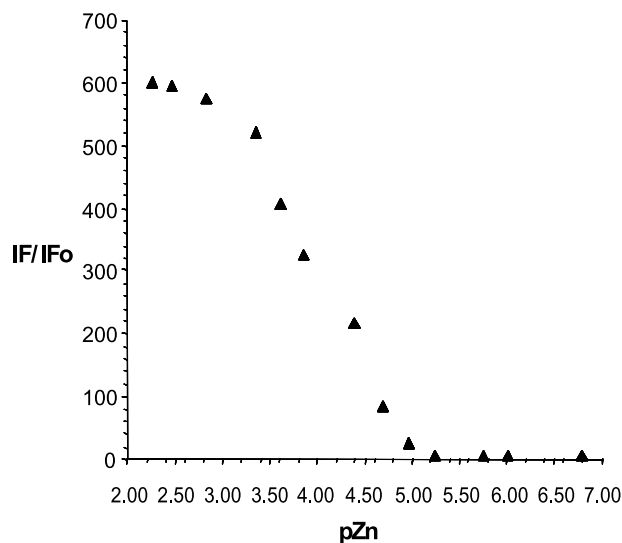


Figure 10. The relative changes in the fluorescence emission of **2** at 415 nm as a function of pZn.

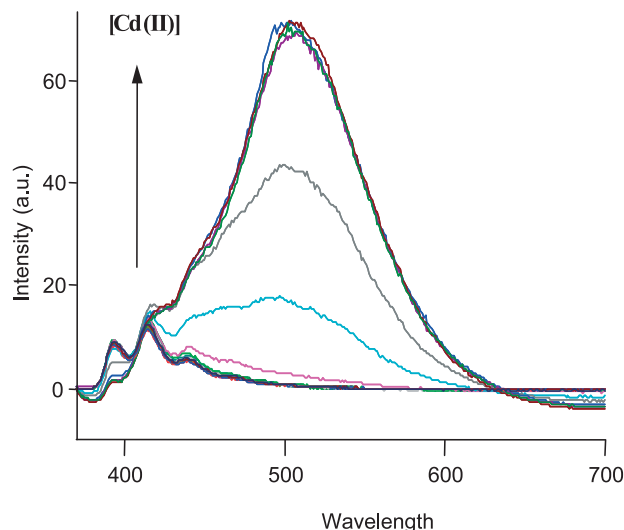


Figure 11. The changes in the fluorescence emission spectra of **1** upon titration with Cd(II).

The corresponding fluorescence emission changes for **1** can be seen in Figure 11. From these changes it is evident that the fluorescence emission is shifted to the red upon Cd(II) recognition, and that the monomeric emission is reduced. Furthermore, in contrast to the changes seen for the Zn(II) titration the emission is substantially more shifted, now centred at 506 nm. Moreover, the fluorescence enhancements are substantially greater than seen for the Zn(II) titration. Again, we suggest that these changes are due to the formation of a charge transfer complex between the anthracene moiety and the bound receptors, in a similar manner to that seen for the Zn(II) titration. As previously demonstrated it was possible to evaluate the binding affinity of **1** towards Cd(II), by plotting the changes at 506 nm as a function of pCd which gave rise to a sigmoidal curve that changed over two pCd units. Fitting these fluorescence

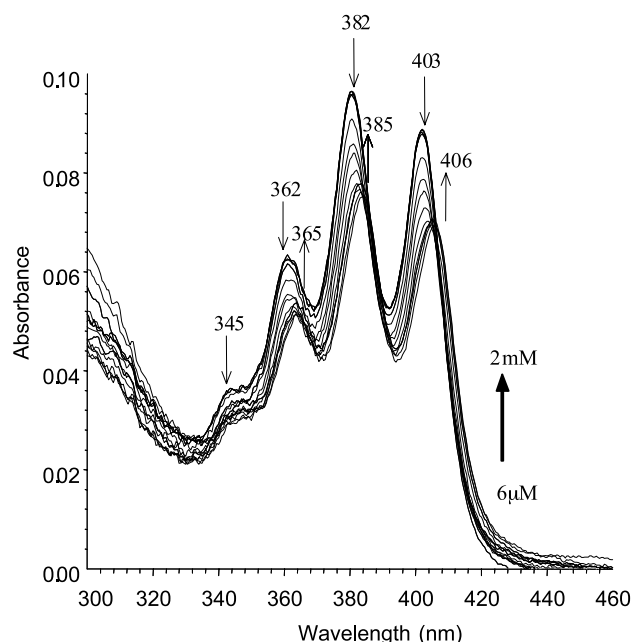


Figure 12. The changes in the UV-Vis spectra of **2**, upon titration with Cd(II).

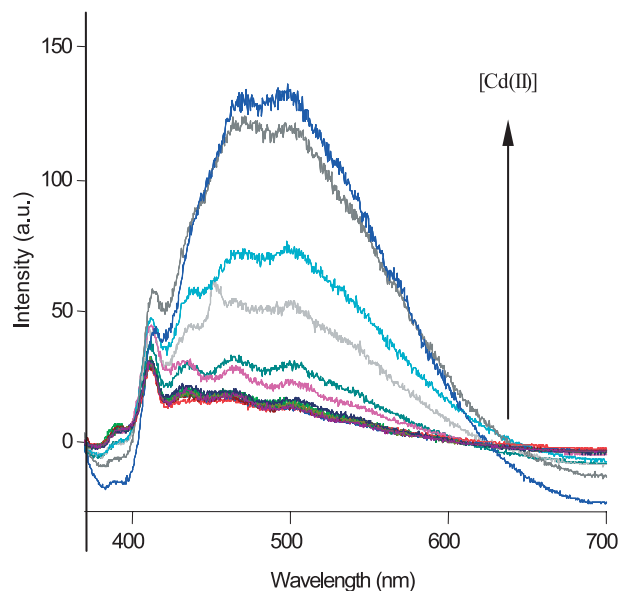


Figure 13. The changes in the fluorescence emission of **2** upon titration with Cd(II).

changes gave a $\log \beta$ of $4.2 (\pm 0.1)$, indicating that selective detection of Cd(II) over Zn(II) should be feasible. Same results were observed when exciting at the isosbestic point.

The fluorescence response of **2** towards Cd(II) was similar to that observed for **1**. However, the absorption spectra were somewhat different to that seen for the Zn(II) titration, as seen in Figure 12. Here the recognition of the ion caused a red shift of ca. 3 nm, with clear isosbestic points being observed at 385 and 405 nm, respectively. From these changes, we were able to determine a binding constant $\log \beta$ of $4.1 (\pm 0.2)$. In contrast to these results the fluorescence emission was red shifted, as shown in Figure 13, with the formation of a broad structure less red shifted band, centred at ca. 500 nm. As explained before, we believe that this is due to the anthracene-Cd(II) charge transfer interaction, in a similar manner to that seen for **1**. The same trends and spectral changes were observed upon excitation at the isosbestic points.

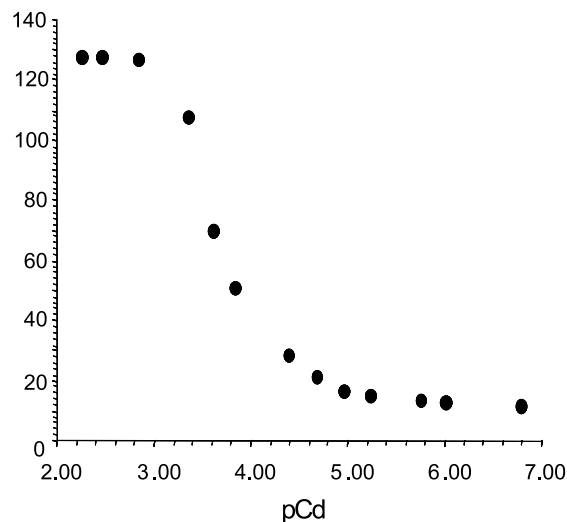


Figure 14. The changes in the fluorescence at 500 nm as a function of pCd.

A plot of fluorescence changes at 500 nm for **2** against pCd(II) resulted in a sigmoidal curve with two logarithmic unit changes, indicating a simple 1:1 equilibrium, Figure 14. From these changes a binding constant $\log \beta$ of $3.9 (\pm 0.1)$ was determined. These results demonstrate that both **1** and **2** can be considered as fluorescence chemosensors for Cd(II), as both have a marginally better selectivity for Cd(II) over that of Zn(II). The binding results are summarised in Table 1.

Table 1

Parameters	1	2
pK _a	1.83 (± 0.1)	2.5 (± 0.1)
Log β Zn(II) _{abs}	—	—
Log β Zn(II) _{flu}	3.8 (± 0.1)	3.8 (± 0.1)
Log β Cd(II) _{abs}	4.0 (± 0.1)	4.1 (± 0.1)
Log β Cd(II) _{flu}	4.2 (± 0.1)	3.9 (± 0.1)

In summary, we have demonstrated efficient fluorescent sensing of Cd(II). For **1**, the sensing of both Zn(II) and Cd(II) gives rise to red shifts in the fluorescence spectra, with relatively little changes in the monomeric emission. However, there is a significant difference between these red shifts, for example, 468 versus 506 nm for Zn(II) and Cd(II) respectively. However, the largest contrast is seen for **2**, where the Zn(II) gives rise to large enhancements in the monomeric anthracene emission, but Cd(II) gives rise to the formation of the charge transfer band at long wavelengths. Consequently, **2** is a particularly attractive chemosensor for Cd(II) as it gives rise to a very different spectral response to different competitive ions. Furthermore, this difference was clearly visible under UV-light ($\lambda_{\text{ex}} = 366$ nm) as at pH 7.4 the emission is switched off, whereas in the presence of Zn(II) and Cd(II) the sensors emits in the blue and green part of the electronic spectrum respectively. When these titrations were repeated using the two esters **4** and **5**, no fluorescence enhancement, or red shift emission was observed, indicating that these molecules were unable to coordinate to these ions. But what gives rise the large red shifted emission upon ion recognition? As we have indicated previously we believe that these are due to charge-transfer interactions between the metal bound receptor and the anthracene moiety. Similar results have recently been reported by Yoon et al.^{9c} and Czarnik et al.^{9h} utilising the anthracene fluorophore and aliphatic Cd(II) based receptors. Both researchers suggested that their anthracene–Cd(II) interactions were initially due to π -complex formation, which then gave rise to the formation of a σ -complex. However, for both of these examples the fluorescence emission was centred on 446 nm. This is a significantly smaller red shift than observed for either **1** and **2** upon recognition of Cd(II). Although, we do not predict that such σ -complex interaction can occur for either **1** or **2**, solely due to steric effects, as we, unlike Yoon et al. and Czarnik et al.^{9h} use aromatic based receptors, the formation of the long emitting emission bands for both **1** and **2** strongly suggest the formation of π -complex interactions. Moreover, as the concentration of the sensor used in the titration studies is very low (1 μ M), intermolecular exciplex, excimer and mixed excimer formation can be effectively ruled out. To the best of our knowledge, **1** and **2** are the first examples of highly

selective fluorescent chemosensors for Cd(II), that can operate under physiological pH conditions.

2.5. Competitive Cd(II) measurements of **1** and **2**

To confirm the selectivity of **2** towards Cd(II) over Zn(II), we performed a Cd(II) titration in the presence of excess Zn(II). These results are summarised in Figure 15. A 1 μ M solution of **2** was prepared in HEPES buffer at pH 7.4. Under this condition the emission can be said to be switched off. This solution was adjusted to contain 3 mM of Zn(II), which caused normal fluorescence emission to be switched on. This Zn(II)-**2** solution was then titrated with Cd(II) in the same manner as described above. As predicted the addition of Cd(II) induced a shift to longer wavelength with the appearance of a new broad band at 500 nm, demonstrating that **2** is capable of selectively signalling the presence of Cd(II) over Zn(II). Similar effects were seen for **1**, where the emission further red shifted upon addition of Cd(II) to a solution of Zn(II). These results clearly show the high selectivity that these sensors have for Cd(II), even in the presence of highly competitive ions such as Zn(II). Its possible that as the binding constants for the two ions is so similar that this selectivity is due to the formation of a more kinetically stable complex in the case of Cd(II).

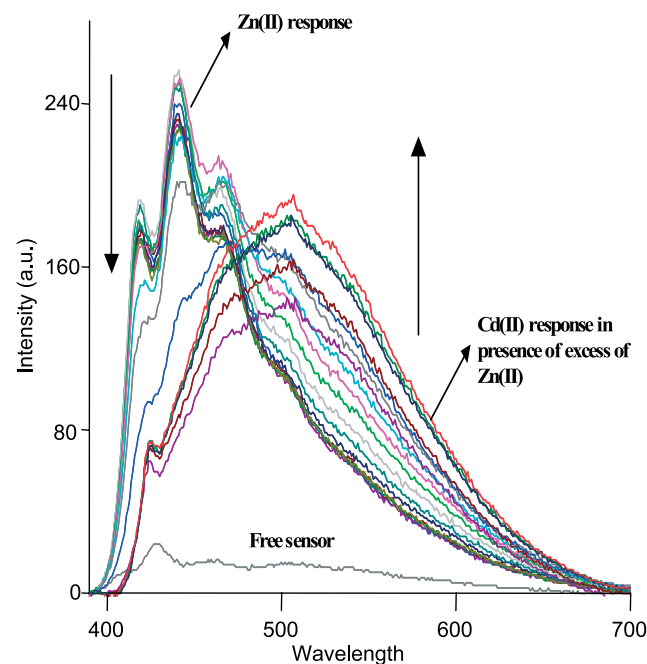


Figure 15. The titration of **2** with Cd(II) ([Cd(II)] 6 mM \rightarrow 2.0 mM) in the presence of 2.0 mM of Zn(II) at pH 7.4.

3. Conclusion

Herein we have presented the results of two novel anthracene based fluorescent chemosensors **1** and **2** for the selective recognition of Cd(II). These were designed on the PET principle, using an anthracene fluorophore, connected to either one or two iminodiacetate receptors via a methylene spacer. These sensors were easily synthesized in two steps from the receptor **3** in a good yield.

The sensors exhibited high pH stability and aqueous solubility, where the fluorescence was switched off above pH ~ 3 , enabling the use of these sensors in competitive pH media such as in physiological pH. The evaluation of the ground and excited state responses of these sensors demonstrated their capability to detect Zn(II) and Cd(II) and to discriminate these ions from group 2 and other transition metal ions. Whereas the recognition of Cd(II) at pH 7.4, gave rise to the formation of charge transfer complexes (σ -complexes) for both sensors (λ_{\max} ca. 506 and 500 nm for **1** and **2** respectively), the recognition of Zn(II) only switched on the (monomeric) anthracene emission of **2**, while for **1** it was red shifted (λ_{\max} = 468 nm). A discrimination test performed to evaluate the selectivity for Cd(II) in the presence of Zn(II) proved very successful, as the monomeric anthracene emission was red shifted upon detection of Cd(II). These results strongly support the possible application of these chemosensors as Cd(II) sensors in physiological samples. This is particularly the case for **2** which exhibits the unique feature of emitting in the blue upon detection of Zn(II), whereas upon the detection of Cd(II) it emits in the green. In this context further evaluation of **2** is required to determine the degree of toxicity, cell permeability and real time response. To the best of our knowledge these are the first examples of such highly selective Cd(II) fluorescent chemosensors.

4. Experimental

4.1. General

Starting materials were obtained from Sigma Aldrich, Strem Chemicals and Fluka. Columns were run using silica gel 60 (230–400 mesh ASTM) or aluminum oxide (activated, Neutral, Brockmann I STD grade 150 mesh). Solvents were used at GPR grade unless otherwise stated. Infrared spectra were recorded on a Mattson Genesis II FTIR spectrophotometer equipped with a Gateway 2000 4DX2-66 workstation. Oils were analysed using NaCl plates, solid samples were dispersed in KBr and recorded as clear pressed discs. ^1H NMR spectra were recorded at 400 MHz using a Bruker Spectrospin DPX-400 instrument. Tetramethylsilane (TMS) was used as an internal reference standard, with chemical shifts expressed in parts per million (ppm or δ) downfield from the standard. ^{13}C NMR were recorded at 100 MHz using a Bruker Spectrospin DPX-400 instrument. Mass spectroscopy was carried out using HPLC grade solvents. Mass spectra were determined by detection using Electrospray on a Micromass LCT spectrometer, using a Shimadzu HPLC or Water's 9360 to pump solvent. The whole system was controlled by MassLynx 3.5 on a Compaq Deskpro workstation.

4.1.1. [(4-Anthracen-9-ylmethyl-phenyl)-ethoxycarbonyl-methyl-amino]-acetic acid ethyl ester (4). 9-Chloromethylantracene (1.5 g, 6.64 mmol) and phenyliminodiacetic acid diethyl ester (**3**) (1.76 g, 6.64 mmol) and AlCl_3 (0.91 g, 6.64 mmol) were dissolved in dry CHCl_3 (50 mL) at -5°C . The solution was refluxed overnight. After the reaction was complete (monitoring by TLC) the solution was cooled and washed with three 100 mL portions of water. The organic portion was dried over MgSO_4 . After

evaporation of the solvent, crude product was subjected to column chromatography using ethyl acetate/hexane (2:3) as eluant to yield pure **4** (1.89 g, 70%) as light yellow thick liquid. Mp = $140\text{--}142^\circ\text{C}$. MS (ES^+) m/z = 456 (MH^+). Anal. Calcd for $\text{C}_{29}\text{H}_{29}\text{NO}_4$: C, 76.46; H, 6.42; N, 3.07. Found: C, 76.18; H, 6.28; N, 3.07. ^1H NMR (400 MHz, CDCl_3): δ , 1.25 (t, 6H, J = 7.0 Hz, $\text{NH}_2\text{CH}_2\text{CO}_2\text{CH}_2\text{CH}_3$), 4.07 (s, 4H, $\text{NCH}_2\text{CO}_2\text{CH}_2\text{CH}_3$), 4.18 (q, 4H, J = 7.0 Hz, $\text{NCH}_2\text{CO}_2\text{CH}_2\text{CH}_3$), 4.92 (s, 2H, CH_2), 6.47 (d, 2H J = 8.5 Hz, Ar-H), 6.98 (d, 2H, J = 8.5 Hz, Ar-H), 7.45–7.48 (m, 4H, Ar-H), 8.03–8.05 (m, 2H, Ar-H), 8.22–8.25 (m, 2H, Ar-H), 8.43 (s, 1H, Ar-H). ^{13}C NMR (100 MHz, CDCl_3): δ , 170.50, 145.68, 132.03, 130.12, 130.04, 131.24, 128.57, 128.45, 125.82, 125.26, 124.54, 124.40, 112.26, 60.53, 53.06, 32.02, 13.72. IR (ν_{\max} , NaCl, cm^{-1}): 3345, 2977, 1895, 1931, 1854, 1765, 1676, 1615, 1568, 1521, 1480, 1447, 1386, 1355, 1334, 1274, 1177, 1065, 970, 879, 820, 786, 728, 691, 650, 635, 602, 570, 538, 517.

4.1.2. [(4-Anthracen-9-ylmethyl-phenyl)-ethoxycarbonyl-methyl-amino]-acetic acid potassium salt (1). [(4-Anthracen-9-ylmethyl-phenyl)-ethoxycarbonylmethyl-amino]-acetic acid ethyl ester (**4**) (1 g, 2.19 mmol) was dissolved in methanol (20 mL) while stirring. To this was added aqueous KOH (1 mL, 3 M). The mixture was refluxed for 2 h. After cooling to room temperature, the reaction mixture was kept in the fridge, where the potassium salt precipitated. The resulting solution was filtered and the precipitate dried in vacuum to afford **1** as a pale yellow solid (0.96 g, 95%). Mp = 340°C (decomp.). MS (ES^+) m/z = 476 (MH^+). Anal. Calcd for $\text{C}_{25}\text{H}_{19}\text{KNO}_4 \cdot 2\text{H}_2\text{O}$: C, 58.69; H, 4.53; N, 2.74. Found: 57.80; H, 4.33; N, 2.56. ^1H NMR (400 MHz, D_2O): δ , 3.67 (s, 4H, $\text{NCH}_2\text{CO}_2\text{K}$), 4.65 (s, 2H, CH_2), 6.20 (d, 2H, J = 8.5 Hz, Ar-H), 6.82 (d, 2H, J = 8.5 Hz, Ar-H), 7.36–7.38 (m, 4H, Ar-H), 7.91 (d, 2H, J = 5.5 Hz, Ar-H), 8.12 (d, 2H, J = 6.0 Hz, Ar-H), 8.30 (s, 1H, Ar-H). ^{13}C NMR (100 MHz, D_2O): δ , 177.61, 144.74, 131.10, 129.26, 127.61, 126.89, 126.68, 126.55, 124.06, 123.95, 123.20, 122.57, 109.48, 53.54, 29.22. IR (ν_{\max} , KBr, cm^{-1}): 3400, 2877, 2844, 1964, 1915, 1723, 1660, 1500, 1445, 1336, 1256, 1186, 519, 535, 564, 601, 618, 656, 697, 758, 790, 819, 852, 1158, 1100, 987, 955, 903, 884.

4.1.3. [(4-{10-[4-(Bis-ethoxycarbonylmethyl-amino)-benzyl]-anthracen-9-ylmethyl}-phenyl)-ethoxycarbonyl-methyl-amino]-acetic acid ethyl ester (5). 9,10-Bischloromethyl anthracene (1.0 g, 3.63 mmol), phenyliminodiacetic acid diethyl ester (**3**) (1.93 g, 7.26 mmol) and AlCl_3 (0.96 g, 7.26 mmol) were dissolved in dry CHCl_3 (50 mL) at -5°C . The solution was refluxed under stirring overnight (12 h). After the reaction was complete, (monitored by TLC) the solution was cooled and washed with three 100 mL portions of water. The organic portion was dried over MgSO_4 . After evaporation of the solvent, the crude product was subjected to column chromatography and yielded pure **5** (1.56 g, 58%) as light yellow solid. Mp = $120\text{--}122^\circ\text{C}$. MS (ES^+) m/z = 733 (MH^+). Anal. Calcd for $\text{C}_{44}\text{H}_{48}\text{N}_2\text{O}_8$: C, 72.11; H, 6.60; N, 3.82. Found: C, 72.26; H, 6.45; N, 3.69. ^1H NMR (400 MHz, CDCl_3): δ 1.27 (t, 12H, J = 7.6 Hz, $\text{NCH}_2\text{CO}_2\text{CH}_2\text{CH}_3$), 4.09 (s, 8H, $\text{NCH}_2\text{CO}_2\text{CH}_2\text{CH}_3$), 4.19 (q, 8H, J = 7.0 Hz, $\text{NCH}_2\text{CO}_2\text{CH}_2\text{CH}_3$), 4.95 (s, 4H, CH_2), 6.50 (d, 4H, J = 9.0 Hz, Ar-H), 7.01 (d, 4H, J = 9.0 Hz, Ar-H), 7.44 (m, 4H, Ar-H), 8.27

(m, 4H, Ar-*H*). ^{13}C NMR (100 MHz, CDCl_3 , ppm): δ , 170.52, 145.68, 131.35, 130.25, 130.00, 128.49, 125.19, 124.79, 112.29, 60.54, 53.07, 32.30, 13.74. IR (ν_{max} , KBr, cm^{-1}): 3450, 2979, 1895, 1931, 1859, 1734, 1616, 1568, 1524, 1448, 1371, 1030, 969, 865, 812, 781, 763, 655, 601, 573, 543, 506.

4.1.4. [(4-{10-[4-(Bis-ethoxycarbonylmethyl-amino)-benzyl]-anthracen-9-ylmethyl}-phenyl)-ethoxycarbonylmethyl-amino]-acetic acid potassium salt (2). [(4-{10-[4-(Bis-ethoxycarbonylmethyl-amino)-benzyl]-anthracen-9-ylmethyl}-phenyl)-ethoxycarbonylmethyl-amino]-acetic acid ethyl ester (**5**) (1 g, 1.36 mmol) was dissolved in methanol (20 mL) while stirring. To this aqueous KOH (2 mL, 3 M) was added. The mixture was refluxed for 2 h. After cooling to room temperature the mixture was kept in the fridge, where the potassium salt precipitated out. The resulting solution was filtered and the precipitate dried in vacuum to afford **2** as a pale yellow solid (0.95 g, 90%). Mp = 320 °C (decomp.). MS(ES^+) m/z = 773 ($\text{M} + \text{H}$) $^+$. Anal. Calcd for $\text{C}_{36}\text{H}_{28}\text{K}_4\text{N}_2\text{O}_8 \cdot 3\text{H}_2\text{O}$: C, 52.28; H, 4.14; N, 3.39. Found: C, 52.46; H, 4.02; N, 3.23. ^1H NMR (400 MHz, D_2O): δ , 3.70 (s, 8H, $\text{NCH}_2\text{CO}_2\text{K}$), 4.86 (s, 4H, CH_2), 6.28 (d, 4H, J = 6.1 Hz, Ar-*H*), 6.91 (d, 4H, J = 6.1 Hz, Ar-*H*), 7.42–7.45 (m, 4H, Ar-*H*), 8.29–8.31 (m, 4H, Ar-*H*). ^{13}C NMR (100 MHz, D_2O): δ , 179.22, 146.34, 129.27, 128.41, 128.15, 125.23, 124.95, 111.11, 55.11, 45.30, 31.13. IR (ν_{max} , KBr, cm^{-1}): 3450, 3006, 2005, 1851, 1660, 1574, 1515, 1446, 1404, 1320, 1209, 1043, 1029, 976, 913, 820, 790, 746, 706, 601.

Acknowledgements

We would like to thank TCD, RCSI and HRB for financial support. We also thank Dr. Hazel M. Moncrieff and Dr. John E. O'Brien for their help and discussion. We especially thank Lisa J. Gillespie for her assistance in the preparation of this manuscript.

References and notes

- Rurack, K.; Resch-Genger, U. *Chem. Soc. Rev.* **2002**, *31*, 116. Rurack, K. *Spectrochem. Acta A* **2001**, *57*, 2161. Lavigne, J. J.; Anslyn, E. V. *Angew. Chem., Int. Ed.* **2001**, *40*, 3119. Beer, P. D.; Gale, P. A. *Angew. Chem., Int. Ed.* **2001**, *40*, 486. deSilva, A. P.; Fox, D. B.; Huxley, A. J. M.; Moody, T. S. *Coord. Chem. Rev.* **2000**, *205*, 41. Fabbrizzi, L.; Licchelli, M.; Rabaioli, G.; Taglietti, A. F. *Coord. Chem. Rev.* **2000**, *205*, 85. Czarnik, A. W. *Acc. Chem. Res.* **1994**, *27*, 302.
- Martínez-Máñez, R.; Sancenón, F. *Chem. Rev.* **2003**, *103*, 4419. de Silva, A. P.; Gunaratne, H. Q. N.; Gunnlaugsson, T.; Huxley, A. J. M.; McCoy, C. P.; Rademacher, J. T.; Rice, T. E. *Chem. Rev.* **1997**, *97*, 1515. Czarnik, A. W. *Acc. Chem. Res.* **1994**, *27*, 302. *Fluorescent Chemosensors for Ion and Molecular Recognition*; Czarnik, A. W., Ed.; ACS Books: Washington, 1993. Bissell, R. A.; de Silva, A. P.; Gunaratne, H. Q. N.; Lynch, P. L. M.; Maguire, G. E. M.; McCoy, C. P.; Sandanayake, K. R. A. S. *Top. Curr. Chem.* **1993**, *168*, 223.
- Luminescent devices including employing ion and molecular recognition include: de Silva, A. P.; McCaughan, B.; McKinney, B. O. F.; Querol, M. *Dalton Trans.* **2003**, 1902. Balzani, V. *Photochem. Photobiol. Sci.* **2003**, *2*, 459. Balzani, V.; Credi, A.; Venturi, M. *Pure Appl. Chem.* **2003**, *75*, 541. Raymo, F. M. *Adv. Mater.* **2002**, *14*, 401. Raymo, F. M.; Giordani, S. *J. Am. Chem. Soc.* **2004**, *2002*, 124. Brown, G. J.; de Silva, A. P.; Pagliari, S. *Chem. Commun.* **2002**, 2461. Ballardini, R.; Balzani, V.; Credi, A.; Gandolf, M. T.; Venturi, M. *Acc. Chem. Res.* **2001**, *36*, 445.
- Gunnlaugsson, T.; Lee, C. T.; Parkesh, R. *Org. Biomol. Chem.* **2003**, *1*, 3265. Gunnlaugsson, T.; Kruger, P. E.; Lee, T. C.; Parkesh, R.; Pfeffer, F. M.; Hussey, M. G. *Tetrahedron Lett.* **2003**, *44*, 6575. Gunnlaugsson, T.; Nieuwenhuyzen, M.; Richard, L.; Thoss, V. *J. Chem. Soc., Perkin Trans. 2* **2002**, 141. Gunnlaugsson, T.; Davis, A. P.; Glynn, M. *Org. Lett.* **2002**, *4*, 2449. Gunnlaugsson, T.; Bichell, B.; Nolan, C. *Tetrahedron Lett.* **2002**, *43*, 4989. Gunnlaugsson, T.; Davis, A. P.; Glynn, M. *Chem. Commun.* **2001**, 2556.
- Gunnlaugsson, T.; Kruger, P. E.; Jensen, P.; Pfeffer, F. M.; Hussey, M. G. *Tetrahedron Lett.* **2003**, *44*, 8909. Gunnlaugsson, T.; Kelly, J. M.; Nieuwenhuyzen, M.; O'Brien, A. M. K. *Tetrahedron Lett.* **2003**, *44*, 8571. Gunnlaugsson, T.; Leonard, J. P. *J. Chem. Soc., Perkin Trans. 2* **2002**, 1980. Gunnlaugsson, T.; Nieuwenhuyzen, M.; Richard, L.; Thoss, V. *Tetrahedron Lett.* **2001**, *42*, 4725.
- Gunnlaugsson, T.; Harte, A. J.; Leonard, J. P.; Senechal, K. *J. Am. Chem. Soc.* **2003**, *125*, 12062. Gunnlaugsson, T.; Leonard, J. P. *Chem. Commun.* **2003**, 2424. Gunnlaugsson, T.; Harte, A. J.; Leonard, J. P.; Nieuwenhuyzen, M. *Supramol. Chem.* **2003**, *15*, 505. Gunnlaugsson, T.; Harte, A. J.; Leonard, J. P.; Nieuwenhuyzen, M. *Chem. Commun.* **2002**, 2134. Gunnlaugsson, T.; Mac Dónaill, D. A.; Parker, D. *J. Am. Chem. Soc.* **2001**, *123*, 12866. Gunnlaugsson, T.; Mac Dónaill, D. A.; Parker, D. *Chem. Commun.* **2000**, 93. Gunnlaugsson, T. *Tetrahedron Lett.* **2001**, *42*, 8901.
- Chemical Sensors and Biosensors for Medical and Biological Applications*; Spichiger-Keller, U. C., Ed.; Wiley-VCH: Weinheim, Germany, 1998. *Chemosensors of Ion and Molecular Recognition*; Desvergne, J. P.; Czarnik, A. W., Eds.; Kluwer Academic: Dordrecht, Netherland, 1997.
- He, H.; Mortellaro, M. A.; Leiner, M. J. P.; Fraatz, R. J.; Tusa, J. K. *J. Am. Chem. Soc.* **2003**, *125*, 1468. He, H.; Mortellaro, M. A.; Leiner, M. J. P.; Young, S. T.; Fraatz, R. J.; Tusa, J. K. *Anal. Chem.* **2003**, *75*, 549.
- (a) Costero, A. M.; Andreu, R.; Monrabal, E.; Martinez-Manez, R.; Sancenón, F.; Soto, J. *J. Chem. Soc., Dalton Trans.* **2002**, 1769. (b) Prodi, L.; Montalti, M.; Zaccaroni, N.; Bradshaw, J. S.; Izatt, R. M.; Savage, P. B. *Tetrahedron Lett.* **2001**, *42*, 2941. (c) Choi, M.; Kim, M.; Lee, K. D.; Han, K. N.; Yoon, I. A.; Chung, H. J.; Yoon, J. *Org. Lett.* **2001**, *3*, 3455. (d) Charles, S.; Yunus, S.; Dubois, F.; Vander Donckt, E. *Anal. Chim. Acta* **2001**, *440*, 37. (e) Ertas, N.; Akkaya, E. U.; Ataman, O. Y. *Talanta* **2000**, *51*, 693. (f) Prodi, L.; Bolletta, F.; Montalti, M.; Zaccaroni, N. *Eur. J. Inorg. Chem.* **1999**, *3*, 455. (g) Lu, J. Z.; Zhang, Z. *J. Analyst* **1995**, *120*, 453. (h) Huston, M. E.; Engleman, C.; Czarnik, A. W. *J. Am. Chem. Soc.* **1990**, *112*, 7054.
- Some of our preliminary work was recently published: Gunnlaugsson, T.; Lee, C. T.; Parkesh, R. *Org. Lett.* **2003**, *5*, 4065.
- Cadmium and Compounds*, US Environmental Protection Agency, 2001.
- Frausto da Silva, J. J. R.; Williams, R. J. In *The Biological*

- Chemistry of the Elements: The Inorganic Chemistry of Life*, 2nd ed.; Oxford University Press: Oxford, 2001. *CRC Handbook of Chemistry and Physics*, 77th ed., CRC: Boca Raton, Florida, 1996. Carr, D. S. Cadmium and Cadmium Alloys, 4th ed. In *Kirk-Othmer Encyclopaedia of Chemical Technology*, Vol. 4; Wiley: New York, 1992.
13. Dobson, S. *Cadmium-Environmental Aspects*; World Health Organisation: Geneva, 1992. Jackson, T.; MacGillivray, A. In *Accounting for Cadmium*; Stockholm Environment Institute: London, 1993. Jones, R.; Lapp, T.; Wallace, D. In *Locating and Estimating Air Emissions from Sources of Cadmium and Cadmium Compounds*, Institute for the US Environment Protection Agency, Office of Air and Radiation, Report EPA-453/R-93-040, **1993**.
14. Rydh, C. J.; Svärd, B. *Sci. Total Environ.* **2003**, 302, 167.
15. Benjamin, M. W.; Honeyman, B. D. In *Global Biogeochemical Cycles*; Butcher, S. S., Charlson, R. J., Orians, G. H., Wolfe, G. V., Eds.; Academic: London, 1992; p 317.
16. Nordberg, G. F.; Nordberg, M. In *Biological Monitoring of Trace Metals*; Clarkson, T. W., Friberg, L., Nordberg, G. F., Sager, P. R., Eds.; Plenum: New York, 1998; Vol. 151.
17. Falnoga, I.; Tusek-Znidaric, M.; Horvat, M.; Stegnar, P. J. *Environ. Pathol. Toxicol. Oncol.* **2000**, 19, 201.
18. Regunathan, A.; Glesne, D. A.; Wilson, A. K.; Song, J.; Nicolae, D.; Flores, T.; Bhattacharyya, M. H. *Toxicol. Appl. Pharmacol.* **2003**, 191, 272.
19. Nakadaira, H.; Nishi, S. *Sci. Total Environ.* **2003**, 309, 48.
20. de Silva, A. P.; Sandanayake, K. R. A. S. *Angew. Chem., Int. Ed.* **1990**, 29, 1173. de Silva, A. P.; de Silva, S. A. *J. Chem. Soc., Chem. Commun.* **1986**, 1709.
21. Structurally similar receptors have been used for the detection of Mg^{2+} : de Silva, A. P.; Gunaratne, H. Q. N.; Maguire, G. E. M. *J. Chem. Soc., Chem. Commun.* **1994**, 1213; and for Zn(II): Reany, O.; Gunnlaugsson, T.; Parker, D. J. *Chem. Soc., Perkin Trans. 2* **2000**, 1819.
22. Burdette, S. C.; Walkup, G. K.; Spingler, B.; Tsien, R. Y.; Lippard J. *Am. Chem. Soc.* **2001**, 123, 7831.
23. Bhattacharyya, K.; Chowdhury, M. *Chem. Rev.* **1993**, 93, 507.
24. Cloninger, M. J.; Whitlock, H. W. *J. Org. Chem.* **1998**, 63, 6153.